

## Neuronal morphometry directly from bitmap images

Tiago A Ferreira<sup>1</sup>, Arne V Blackman<sup>2</sup>, Julia Oyrer<sup>2</sup>, Sriram Jayabal<sup>3</sup>, Andrew J Chung<sup>1</sup>, Alanna J Watt<sup>4</sup>, P Jesper Sjöström<sup>1,2</sup>, and Donald J van Meyel<sup>1,4</sup>

<sup>1</sup>Centre for Research in Neuroscience, Department of Neurology and Neurosurgery, The Research Institute of the McGill University Health Centre, Montreal, Quebec, Canada

<sup>2</sup>Department of Neuroscience, Physiology, and Pharmacology, University College London, London, UK

<sup>3</sup>McGill Integrated Program in Neuroscience, Montreal, Quebec, Canada

<sup>4</sup>Department of Biology, McGill University, Montreal, Quebec, Canada

---

### To the Editor

Neuroscientists measure the tree-like structures of neurons in order to better understand how neural circuits are constructed and how neural information is processed. In 1953, Donald Sholl published his well-known technique for quantitative analysis of the complex arbors of dendrites and axons<sup>1</sup>, but conventional methods still require their reconstruction via time-consuming manual or semi-automated tracing from microscopy images. To bypass this reconstruction step and perform the Sholl technique directly on images instead, we developed Sholl Analysis, an open-source program for ImageJ/Fiji<sup>2</sup> (Supplementary Fig. 1). The plug-in employs an improved algorithm to retrieve data from two- or three-dimensional (2D or 3D) bitmap images in any format supported by the Bio-Formats library (Supplementary Methods). It pairs this data retrieval with curve-fitting, regression analysis and statistical inference so that users can automatically extract a collection of Sholl-based metrics of arborization<sup>1,3</sup> (Supplementary Note).

Using individual cortical pyramidal neurons in 3D images, we found Sholl Analysis to be accurate when benchmarked against corresponding manual reconstructions (Supplementary Fig. 2). The method was also resilient to image degradation by simulated shot noise (Supplementary Fig. 3). To further assess accuracy, and to explore the utility of Sholl Analysis in tackling neurons that are particularly slow to reconstruct manually, we studied cerebellar Purkinje cells in mice, which have large and intricate dendritic arbors. From tiled 3D image stacks of cerebellum (Fig. 1a), we selected seven Brainbow2.1-expressing

---

Note: Any Supplementary Information and Source Data files are available in the online version of the paper (doi:10.1038/nmeth.3125).

#### AUTHOR CONTRIBUTIONS

T.A.F. developed the software and analyzed the data. A.V.B., J.O. and A.J.C. provided image data and manual reconstructions of neocortical cell morphologies. A.J.W. collected Brainbow images and S.J. manually reconstructed individual Brainbow-labeled Purkinje cells. P.J.S. and D.J.v.M. provided guidance. T.A.F., A.J.W., P.J.S. and D.J.v.M. wrote the manuscript.

#### COMPETING FINANCIAL INTERESTS

The authors declare no competing financial interests.

Purkinje neurons and isolated their morphologies (Fig. 1b and Supplementary Note). We then used the Sholl Analysis software to retrieve ten metrics and found they were indistinguishable from those retrieved from manual reconstructions of the same 7 cells (Fig. 1c,d and Supplementary Methods).

To probe the sensitivity of the Sholl Analysis software, we asked whether its metrics could be used to distinguish closely-related neocortical interneuron subtypes. Parvalbumin-positive (PV) interneurons in layer 5 of visual cortex can be morphologically classified into two subtypes on the basis of their axonal morphology: type 1 PV cells have ascending axons arborizing in layer 2/3, whereas axons of type 2 cells remain in layer 5 (ref. 4). Because their dendritic arbors are indistinguishable<sup>4</sup>, these two cell types otherwise appear highly similar (Fig. 1e–f). Using the Sholl Analysis software, we retrieved 18 metrics directly from 3D image stacks of 12 PV interneurons. We then used Ward's hierarchical clustering based on these metrics to independently classify these cells (Fig. 1g and Supplementary Fig. 4). The 12 cells segregated into two groups: one group of five neurons and another of seven. We found that all the neurons but two were correctly classified, with one cell assigned incorrectly to each class (Fig. 1g). Thus, our use of the Sholl Analysis software to quantify arborization directly from bitmap images correctly identified 80–86% of cells. In agreement, linear Sholl plots of type 1 cells indicated more branching than was found for type 2 cells at a distance of 225–300  $\mu\text{m}$  from the soma (Fig. 1h), which corresponds to their characteristic axonal arborization in upper cortical layers.

The Sholl Analysis software can be applied universally to gray-scale images of neurons of different shapes or sizes provided that they can be distinguished spatially or spectrally. It can be used in synergy with additional tools that sample bitmap images directly, such as skeletonization algorithms (<http://fiji.sc/Strahler>) to automate the hierarchical ordering of branches within arbors<sup>5</sup>. Outside neuroscience, it could also be used to measure other branched structures with a defined focus, such as retinal vasculature or mammary ducts (Supplementary Note). In our experience, the software required only 10–15 min of processing for each of the analyzed PV inter-neurons, whereas manual reconstructions of such cells typically take 3–4 h<sup>4</sup>, and longer yet for Purkinje cells. Batch processing capabilities make Sholl Analysis scalable for large data sets and suitable for high-throughput studies in which images can be analyzed with minimal or automated preprocessing. Because it bypasses reconstruction entirely, morphometry directly from bitmap images is an efficient method for quantification of neuronal arbors and classification of cells.

## Supplementary Material

Refer to Web version on PubMed Central for supplementary material.

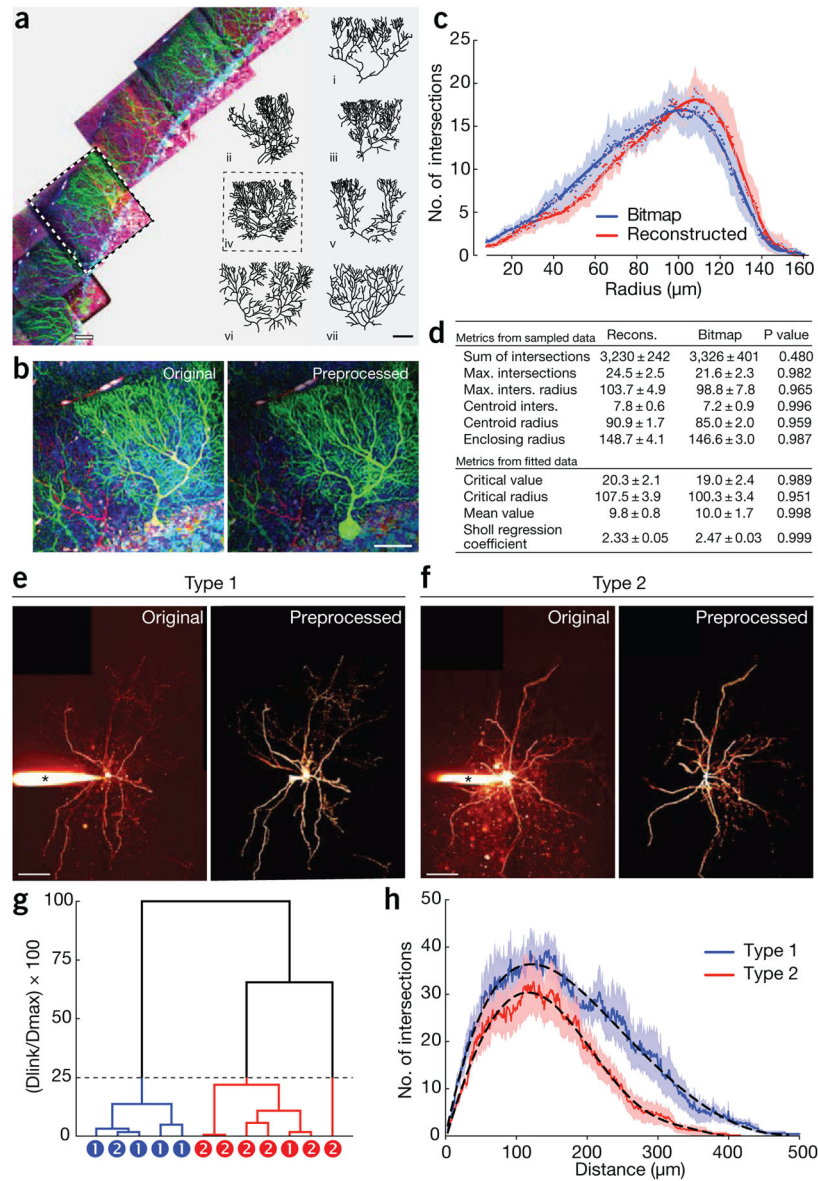
## Acknowledgments

The authors thank T. Maddock for implementing version 1.0 of the software. We also thank J. Schindelin, W. Rasband and M. Longair for code contributions, H. Nedelcescu for deconvolution and alignment of Brainbow images before reconstruction, and B. Chen for advice. Work supported by operating and infrastructure grants to A.J.W., P.J.S. and D.J.v.M. from the Canadian Institutes of Health Research (CIHR), the Natural Sciences and Engineering Research Council of Canada, the Canada Foundation for Innovation and the UK Medical Research Council. Salary awards came from the Research Institute of McGill University Health Center (T.F.), the McGill Faculty of Medicine

(D.J.v.M.), a Biotechnology and Biological Sciences Research Council Industrial CASE studentship (A.V.B.), a University College London Impact Award (J.O.), and a CIHR New Investigator Award (P.J.S.).

## References

1. Sholl DA. *J Anat.* 1953; 87:387–406. [PubMed: 13117757]
2. Schindelin J, et al. *Nat Methods.* 2012; 9:676–682. [PubMed: 22743772]
3. Ristanovi D, et al. *J Neurosci Methods.* 2006; 158:212–218. [PubMed: 16814868]
4. Buchanan KA, et al. *Neuron.* 2012; 75:451–466. [PubMed: 22884329]
5. Strahler AN. *Geol Soc Am Bull.* 1952; 63:1117.

**Figure 1.**

Sholl Analysis provides metrics of complex arbors in Brainbow-expressing mice and classifies cortical interneurons, without tracing or reconstruction. **(a)** Maximum-intensity projections of tiled image stacks from cerebellar cortex. Reconstructions depict the range of morphologies among the seven Brainbow-labeled Purkinje neurons (i–vii) that were quantified. **(b)** Maximum-intensity projection of the cell highlighted in **a**. Original stacks were preprocessed **(b)** to reduce background and eliminate signal from adjacent cells. **(c)** Linear Sholl plots comparing results for bitmap images to those from manual reconstructions for the seven Purkinje neurons. Dots show the mean, shading the s.e.m., and solid lines the best-fit polynomials (9th order). **(d)** Metrics (mean ± s.e.m.) calculated for bitmap images versus manual reconstructions for the seven Purkinje neurons. *P* values obtained by Student's *t*-test using Holm-Šidák correction. **(e,f)** Maximum-intensity

projections of dye-loaded PV interneurons of type 1 (**e**) or type 2 (**f**). Original stacks were preprocessed to reduce background and eliminate the signal from the recording pipette (\*). (**g**) Dendrogram of Ward's hierarchical clustering of PV interneurons based on Sholl Analysis metrics (see supplementary Fig. 4). Dotted line marks the 25% linkage best cut, and circles note correct PV subtype identities based on manual reconstructions and analysis of axonal projections. (**h**) Linear Sholl plots for type 1 ( $n = 5$ ) versus type 2 ( $n = 7$ ) PV interneurons, showing the mean (solid lines) and s.e.m. (shaded regions). Dashed lines show best-fit polynomials (type 1, 8th degree; type 2, 6th degree). Scale bars: **a,b**, 40  $\mu\text{m}$ ; **e,f**, 100  $\mu\text{m}$ . bitmap images is an efficient method for quantification of neuronal arbors and classification of cells.